COPY NO. 9
RM No. E8I21

NACA RM No. E8I21

RESEARCH MEMORANDUM

SOME EFFECTS OF STATOR CONE ANGLE AND BLADE-TIP LEAKAGE ON 40-PERCENT-REACTION TURBINE HAVING ROTOR-BLADE CAPS

By Robert E. English, Robert J. McCready
and John S. McCarthy

Lewis Flight Propulsion Laboratory
Cleveland, Ohio

NATIONAL ADVISORY COMMITTEE
FOR AERONAUTICS

WASHINGTON
March 23, 1949

NATIONAL ADVISORY COMMITTEE FOR AERONAUTICS

RESEARCH MEMORANDUM

SOME EFFECTS OF STATOR CONE ANGLE AND BLADE-TIP LEAKAGE ON 40-PERCENT-REACTION TURBINE HAVING ROTOR-BLADE CAPS

By Robert E. English, Robert J. McCready
and John S. McCarthy

SUMMARY

For an investigation of the effects of stator cone angle and tip leakage on turbine performance, a single-stage turbine having 40-percent reaction was operated with two stators and two stationary shrouds: (1) a stator having a cone angle of 70° and a stator-blade height 0.92 of the rotor-blade height; (2) a stator having a 0° cone angle and a blade height equal to the rotor-blade height; (3) a labyrinth, no-leakage shroud; and (4) a cylindrical stationary shroud having a radial clearance 0.016 of the blade height. In all cases, the rotor blades were equipped with caps that formed a continuous, cylindrical rotating shroud.

The turbine was operated at an entrance temperature of 660° R with total-pressure ratios from 1.25 to 3.70 and equivalent mean blade speeds from 188 to 855 feet per second. For this range of conditions, the over-all performance of the turbine was determined.

With the 0°-cone-angle stator, the peak brake efficiency was approximately 0.04 higher than with the 70°-cone-angle stator. With the 70°-cone-angle stator, separation probably occurred at the tips of the rotor blades; the separation was eliminated by changing the cone angle to 0° and making the stator-blade height equal to the rotor-blade height. When the labyrinth shroud was replaced by the cylindrical shroud, the efficiency was not changed by a measurable amount.

INTRODUCTION

As part of a program to develop techniques for designing turbines of high efficiency, an investigation is being conducted at

the NACA Lewis laboratory to determine the performance of a single-stage, cold-air turbine in which the relative importance of design variables is evaluated by incorporating systematic changes in the blade design. This investigation should provide data for the design of turbines and indicate where further studies may most profitably be concentrated.

The first phase of this program is an investigation of the effects of stator cone angle and tip leakage on turbine performance. In order to observe the effect of stator cone angle on over-all turbine performance, two stators were used: a stator with a 70° cone angle and a stator-blade height 0.92 of the rotor-blade height; and a stator with a 0° cone angle and a stator-blade height equal to the rotor-blade height. The effect of tip leakage on turbine performance was investigated by operating the turbine with a labyrinth no-leakage shroud and a cylindrical shroud.

Of the possible combinations of these variables, three configurations of the turbine were studied: (1) the 70°-cone-angle stator and the labyrinth shroud; (2) the 0°-cone-angle stator and the labyrinth shroud; and (3) the 0°-cone-angle stator and the cylindrical shroud. For the investigation of these three configurations, the turbine was operated at total-pressure ratios of 1.25 to 3.70 and equivalent mean blade speeds of 188 to 855 feet per second using air at a temperature of 660° R.

SYMBOLS

The following symbols are used in this report:

a	velocity of sound, (ft/sec)
E	turbine-shaft work, (Btu/lb)
g	standard acceleration due to gravity, 32.17 (ft/sec^2)
h	specific enthalpy, (Btu/lb)
J	mechanical equivalent of heat, 778.3 (ft-lb/Btu)
p	absolute pressure, (lb/sq ft)
T	absolute temperature, ($^{\circ}R$)

U mean rotor-blade speed, (ft/sec)

V absolute velocity of gas, (ft/sec)

W gas velocity relative to rotor, (ft/sec)

w weight flow of air, (lb/sec)

α angle of absolute velocity measured from direction of rotor-blade motion, (deg)

β angle of relative velocity measured from direction of rotor-blade motion, (deg)

Δ prefix denoting change

η brake efficiency

ρ mass density, (slug/cu ft)

Subscripts:

0 NACA sea-level air; 2116 (lb/sq ft) and 518.4° R

1 stator entrance

2 rotor entrance

3 rotor exit

j ideal jet

s isentropic

u tangential component

x axial component

Superscript:

' total, or stagnation, state

TURBINE DESIGN

The aerodynamic design of the turbine is for the following conditions:

[redacted]

Entrance absolute total temperature, T_1', °R	1960
Entrance absolute total pressure, p_1', lb/sq ft	2829
in. Hg	40
Mean rotor-blade speed, U, ft/sec	1210
Total-to-static pressure ratio, p_1'/p_3,	4.0
Amount of reaction, $\frac{A_s h_{2,3}}{(h_1' - h_3)_s}$	0.40

Because the experimental investigation was conducted at a low turbine-entrance temperature (660° R) as contrasted with the design conditions and because the performance data are expressed in terms of the entrance and exit total states, blade speed and pressure ratio are more conveniently stated in terms of equivalent mean blade speed at NACA sea-level air conditions and total-pressure ratio. The design conditions correspond to an equivalent mean blade speed $U\left(\frac{a_0}{a_1'}\right)$ of 645 feet per second and a total-pressure ratio p_1'/p_3' of 3.32. The velocity-vector diagram for the mean section is given in figure 1. The turbine was designed for a stator exit angle α_2 of 20°, a constant along the radius. Upstream of the stator, downstream of the rotor, and in the axial clearance space between the stator and the rotor, both the static pressure and the mass flow per unit of annulus area were assumed to be constant along the radius. The expansion in the turbine was assumed to be adiabatic, and the working fluid was assumed to have a ratio of specific heats equal to 1.300 and a specific heat at constant pressure equal to 0.300.

The turbine wheel was composed of 150 blades that were 1.50 inches long; the mean diameter midway between the rotor entrance and exit was 13.25 inches and the outer wheel diameter, 14.75 inches. (See fig. 2.) The blades were die-cast aluminum, each with an integral cap at the tip, so that with the blades clamped between two disks the caps formed a continuous, rotating shroud. (See fig. 3.) The rotor-blade profile is shown in figure 4.

Stators

A stator (fig. 5) was available from another turbine whose rotor diameters and blade height were the same as those of the experimental turbine; in addition, the trailing-edge angle of the stator blades was equal to 20°. If the assumptions used in designing the rotor blades are applied to this stator and the effects of rotor-blade overlap are neglected, the stator meets the design conditions at the entrance to the rotor. The stator had a cone angle of 70° and

contained 28 stator blades. The stator-blade height was about 1/8 inch less than the blade height at the rotor entrance, or 0.92 of the rotor-blade height. This stator was cast in one piece.

A second stator (fig. 6), which was of welded construction, had a 0° cone angle, and contained 36 stator blades. The stator-blade height was made equal to the blade height at the rotor entrance. If the assumptions used in designing the rotor blades are applied to this stator, the stator meets the design conditions at the rotor entrance.

Four differences existed in the two stators; namely, the method of construction, the number of stator blades, the cone angle, and the stator-blade height. The internal surfaces of the 70°-cone-angle stator were hand-finished so that the surfaces of both stators were of approximately equal roughness. Because the solidity is high and separation is unlikely to occur in either stator, the number of stator blades should have little effect. The cone angle and the stator-blade height are the significant differences. With each stator, the minimum axial clearance between the stator blades and the rotor blades was between 0.120 and 0.140 inch.

Shrouds

The two shrouds used in this investigation are shown in figure 7. The labyrinth, no-leakage, stationary shroud (fig. 7(a)) consists of a circular ring with two circumferential grooves on the inner surface. The radial clearance between the labyrinth stationary shroud and the cylindrical rotating shroud formed by the blade caps is 0.025 inch. Leakage between the labyrinth shroud and the blade caps was prevented by introducing air into the space downstream of the labyrinth shroud. The amount of labyrinth-sealing air was so adjusted that the pressures in the two circumferential grooves were equalized; when the pressures were equal, it was assumed that no air leaked past the shroud.

The cylindrical stationary shroud (fig. 7(b)) is the same width as the blade caps. The radial clearance between the blade caps and the shroud was 0.025 inch, or 0.016 of the blade height.

Configurations

The three turbine configurations investigated are shown in figure 8. Configuration 1 includes the 70°-cone-angle stator and

the labyrinth stationary shroud; configuration 2, the 0°-cone-angle stator and the labyrinth stationary shroud; and configuration 3, the 0°-cone-angle stator and the cylindrical stationary shroud.

APPARATUS AND PROCEDURE

Experimental Equipment

The arrangement of the experimental equipment is diagrammatically shown in figure 9. Room air enters the electrostatic precipitator where dust particles are removed and passes through a submerged flat-plate orifice, an automatically controlled steam-supplied air heater, a surge tank, and into a pair of ducts leading to the plenum chamber immediately upstream of the turbine stator. The air-flow path from the plenum chamber through the turbine is shown in figure 10 with the labyrinth shroud and the 70°-cone-angle stator of configuration 1 installed in the turbine. Air entering the plenum chamber passes through an 18-mesh, 27-gage screen, turns, and flows through a straightening grid. The air then passes through the stator and the rotor and leaves the turbine through the annular passage between the two exhaust-guide shells coaxially mounted in the tail pipe. The space between the outer guide shell and the tail pipe is provided to carry off the sealing air supplied to the labyrinth.

Downstream of the turbine, the air flows through a large surge tank into a low-pressure exhaust system (fig. 9). The air pressure drop across the turbine is controlled by a butterfly valve downstream of the second surge tank. A 300-horsepower water brake, cradle-mounted for torque measurements, was used for power absorption.

Instrumentation

The location of the turbine instrumentation is shown in figure 10. Entrance total pressure p_1' was indicated by a total-pressure tube 3/4 inch upstream of the stator blades; the entrance total temperature T_1' was measured with thermocouples at four stations within the pair of ducts leading to the plenum chamber. The exit static pressure p_3 was measured by six wall taps located in the exhaust-guide shells downstream of the rotor. The exit total temperature T_3' was measured by three total-temperature thermocouples at the downstream end of the two exhaust-guide shells.

Water-brake torque was indicated by an NACA balanced-diaphragm dynamometer-torque indicator (reference 1). Air flow w was measured by the 7-inch submerged flat-plate orifice upstream of the air heater (fig. 9). Turbine speed was indicated by a calibrated electric tachometer.

The accuracy in reading the data may be summarized as follows:

(1) Absolute pressure, ±0.05 inch of mercury
(2) Temperatures, ±1° R
(3) Orifice pressure drop, ±0.05 inch in a range with a minimum of 15 inches
(4) Torque, ±0.05 inch in a range with a minimum of 17 inches
(5) Rotative speed, ±13 rpm in a range with a minimum of 3700 rpm

An estimate of the reproducibility of the measurements indicates that the probable variation in the brake efficiency for a single data point is less than 0.01 for total-pressure ratios p_1'/p_3' greater than 2.00.

Experimental Procedure

Data were taken at turbine speeds from 3700 to 16,800 rpm (equivalent mean blade speeds from 188 to 855 ft/sec) at total-pressure ratios p_1'/p_3' from 1.25 to 3.70. At each of ten pressure ratios, the turbine was operated at six to ten different speeds. For all runs the entrance total temperature was held between 658° and 662° R; the entrance total pressure varied with the air flow and the barometric pressure between $26\frac{1}{2}$ and 28 inches of mercury.

PERFORMANCE CALCULATIONS

All turbine performance data were reduced to NACA sea-level air conditions at the turbine entrance. The performance was determined in terms of the following variables:

(1) Brake efficiency, η
(2) Total-pressure ratio, p_1'/p_3'
(3) Equivalent turbine-shaft work, $E\left(\frac{a_0}{a_1}\right)^2$
(4) Equivalent mean rotor-blade speed, $U\left(\frac{a_0}{a_1}\right)$

(5) Ratio of equivalent mean rotor-blade speed to equivalent mass flow, $\frac{U\rho_1'}{w\rho_0}$ (This is the reciprocal of mass flow per unit blade speed.)

(6) Ratio of mean rotor-blade speed to ideal jet speed (blade-to-jet speed ratio), U/V_j

The brake efficiency of the turbine, which includes the mechanical efficiency of the turbine, is defined as

$$\eta = \frac{E}{\Delta_s h_{1,3'}}$$

The weight flow of air w was determined from the orifice measurements and the data of reference 2.

The ideal enthalpy drop $\Delta_s h_{1,3'}$ was computed using the chart of air properties in reference 3 and the values of entrance total pressure and temperature and exit total pressure, p_1', T_1', and p_3', respectively. Because the exit total pressure p_3' was not directly measured, this value was computed. The exit static pressure p_3, the exit total temperature T_3', the weight flow w, and the annular area between the exhaust-guide shells were used to determine the exit total pressure p_3' by adding to the measured static pressure a dynamic pressure computed from continuity with the assumptions that the tangential velocity is zero and the axial velocity is constant; these assumptions result in efficiency values that are always conservative.

The ideal jet speed V_j is the jet speed for an isentropic expansion from the entrance total state to the exit static pressure, that is,

$$V_j = \sqrt{2Jg\,(h_1' - h_3)_s}$$

The isentropic enthalpy drop $(h_1' - h_3)_s$ was computed from reference 3 using the entrance total temperature and pressure and the exit static pressure, p_1', T_1', and p_3, respectively.

RESULTS AND DISCUSSION

The performance characteristics over the range of operation covered in this investigation are shown for configurations 1, 2, and 3 in figures 11, 12, and 13, respectively. For each of the

three configurations, the curves of constant equivalent blade speed $U\left(\frac{a_0}{a_1'}\right)$ are vertical above a pressure ratio p_1'/p_3' of approximately 2.25 because the flow through the stator blades was choking and the equivalent weight flow therefore remained constant. The over-all performance characteristics are similar for the three configurations and each configuration has an efficiency near the maximum over the range of pressure ratio from 1.25 to 3.70.

Brake efficiency η plotted against the ratio of blade-to-jet speed ratio U/V_j (fig. 14) is nearly independent of total-pressure ratio p_1'/p_3' for configuration 2. Because this independence of pressure ratio also exists for configurations 1 and 3, the comparison of the three configurations in figure 15 at a pressure ratio of 3.00 is representative of the entire range of pressure ratios. In addition to showing the same changes in brake efficiency as figures 11 to 13, figures 14 and 15 indicate that the maximum brake efficiency was obtained with a blade-to-jet speed ratio U/V_j between 0.50 and 0.55. The maximum brake efficiency was 0.795 for configuration 1 and 0.833 for configuration 2, a difference of approximately 0.04. With the 70°-cone-angle stator, separation probably occurred at the tips of the rotor blades; the performance was improved by changing the cone angle to 0° and making the stator-blade height equal to the rotor-blade height, thereby eliminating the separation (figs. 8(a) and 8(b)). If the efficiency were computed using the total-to-static pressure ratio p_1'/p_3 instead of the total-pressure ratio p_1'/p_3', the relative advantage of configuration 2 over configuration 1 would be substantially unchanged.

For configuration 3 (fig. 8(c)), the maximum brake efficiency was 0.835, an increase of less than 0.005 over the maximum efficiency of configuration 2. Although any tip leakage introduced by replacing the labyrinth no-leakage shroud with the cylindrical shroud would cause a reduction in the working fluid passing through the rotor blades, the measured efficiency slightly increased. Within the probable reproducibility of the data, the performance of configuration 2 is identical to the performance of configuration 3.

In order to determine the approximate magnitude of the leakage air flow between the blade caps and the cylindrical stationary shroud, the weight flow through a thin-plate orifice of equal area was computed and multiplied by a factor of 0.7 (reference 4). The conditions for maximum leakage flow occurred at the highest blade speed and pressure ratio investigated; at these conditions the computed leakage was about 1.7 percent of the air flow entering the turbine. Because the

leakage air flow is mainly from the boundary layer at the outer radius of the flow annulus, this air contains only a small portion of the total energy passing through the turbine.

For configuration 3 (figs. 8(c) and 13), the brake efficiency was 0.82 at the total-pressure ratio and equivalent mean blade speed for which the blades were designed.

SUMMARY OF RESULTS

An investigation of the effects of stator cone angle and blade-tip leakage on turbine performance was conducted with a turbine having 40-percent reaction and a design assumption of constant static pressure over the blade height. Caps at the tips of the rotor blades formed a continuous rotating shroud. The turbine was operated with a turbine-entrance temperature of approximately 660° R at total-pressure ratios from 1.25 to 3.70 and equivalent mean rotor-blade speeds of 188 to 855 feet per second. The following results were obtained:

1. With the 0°-cone-angle stator, the peak brake efficiency was approximately 0.04 higher than with the 70°-cone-angle stator. With the 70°-cone-angle stator, separation probably occurred at the tips of the rotor blades; the performance was improved by changing the cone angle to 0° and making the stator-blade height equal to the rotor-blade height, thereby eliminating the separation.

2. Replacing the labyrinth, no-leakage shroud with a cylindrical stationary shroud that had a radial clearance of 0.016 of the blade height from the cylindrical rotating shroud and using the 0°-cone-angle stator produced no measurable change in brake efficiency.

3. The maximum brake efficiency was obtained with the blade-to-jet speed ratio between 0.50 and 0.55.

Lewis Flight Propulsion Laboratory,
National Advisory Committee for Aeronautics,
Cleveland, Ohio.

REFERENCES

1. Moore, Charles S., Biermann, Arnold E., and Voss, Fred: The NACA Balanced-Diaphragm Dynamometer-Torque Indicator. NACA RB No. 4C28, 1944.

2. Anon.: Fluid Meters, Their Theory and Application. A.S.M.E. Res. Pub., pub. by Am. Soc. Mech. Eng. (New York), 4th ed., 1937.

3. NACA Subcommittee on Compressors: Standard Procedures for Rating and Testing Multistage Axial-Flow Compressors. NACA TN No. 1138, 1946.

4. Stodola, A.: Steam and Gas Turbines. Vol. I. McGraw-Hill Book Co., Inc., 1927, p. 188. (Reprinted, Peter Smith (New York), 1945.)

[redacted]

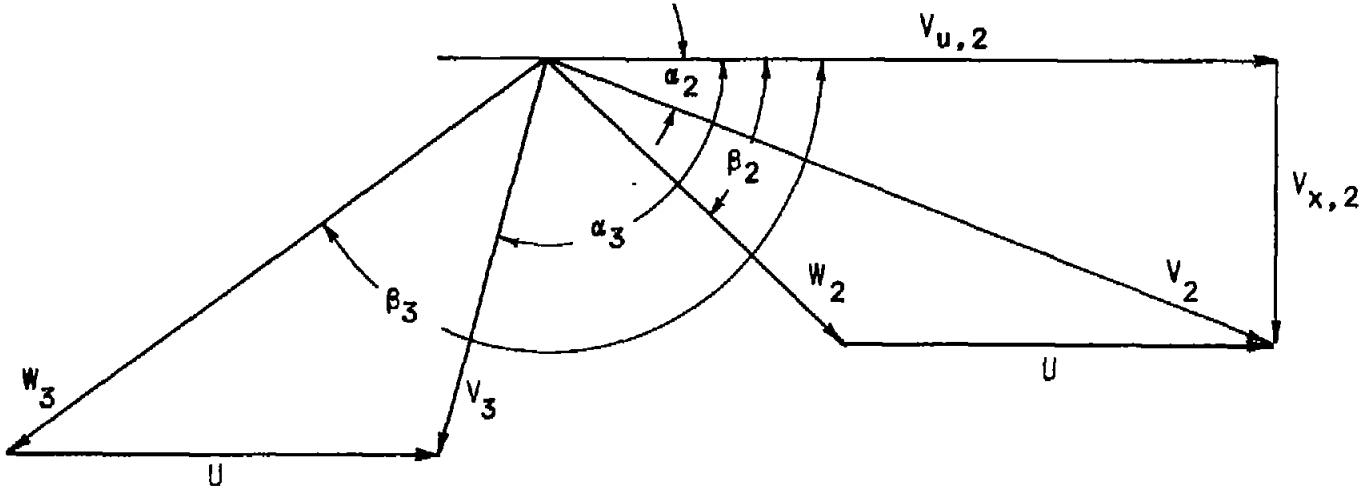

Velocity (ft/sec)		Angle (deg)	
U	1210	α_2	20.0
V_2	2177	α_3	106.4
V_3	1281	β_2	41.7
W_2	1120	β_3	145.5
W_3	2081		

NACA

Figure 1. - Velocity-vector diagram for mean section.

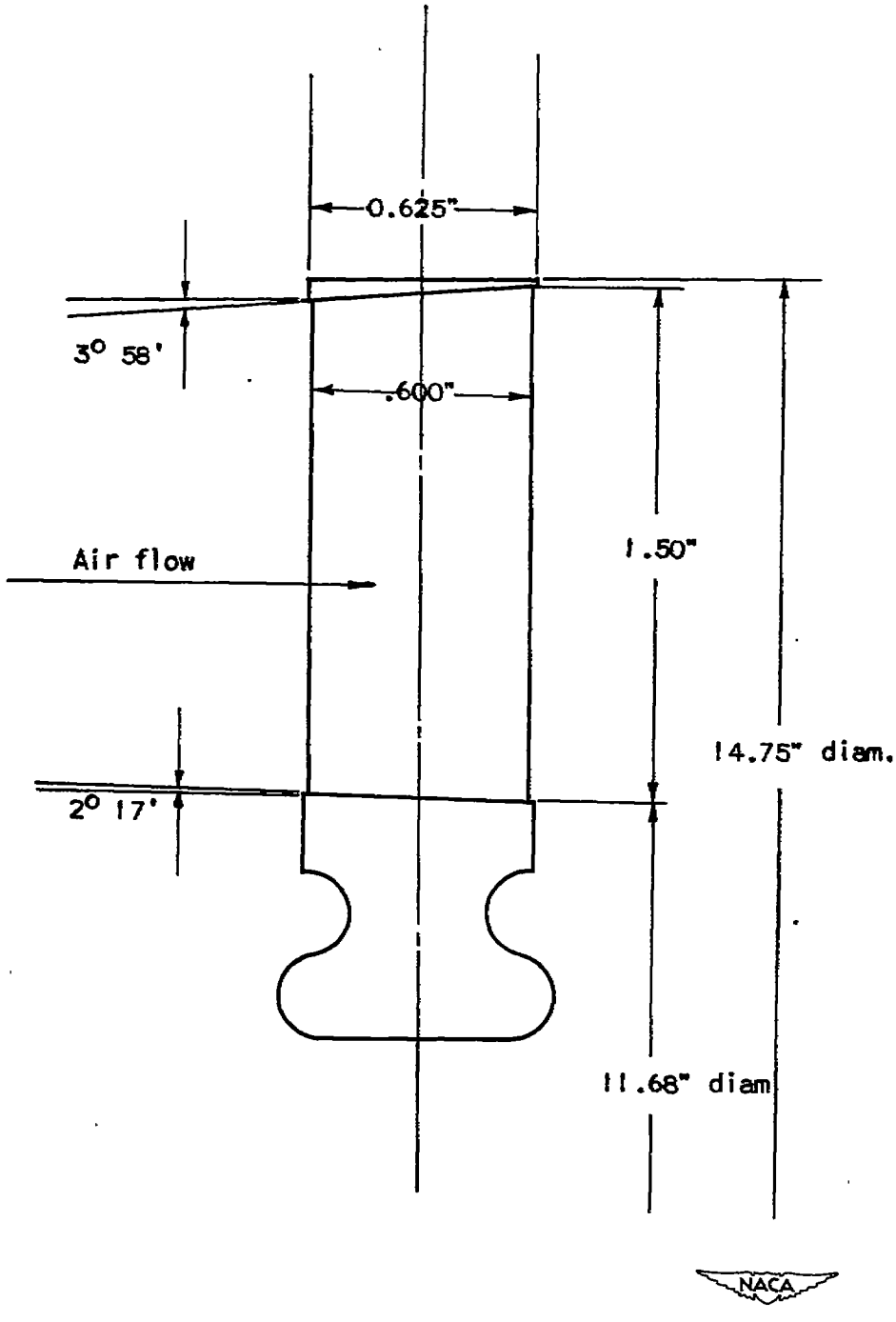

Figure 2. – Sketch of rotor blade showing turbine dimensions.

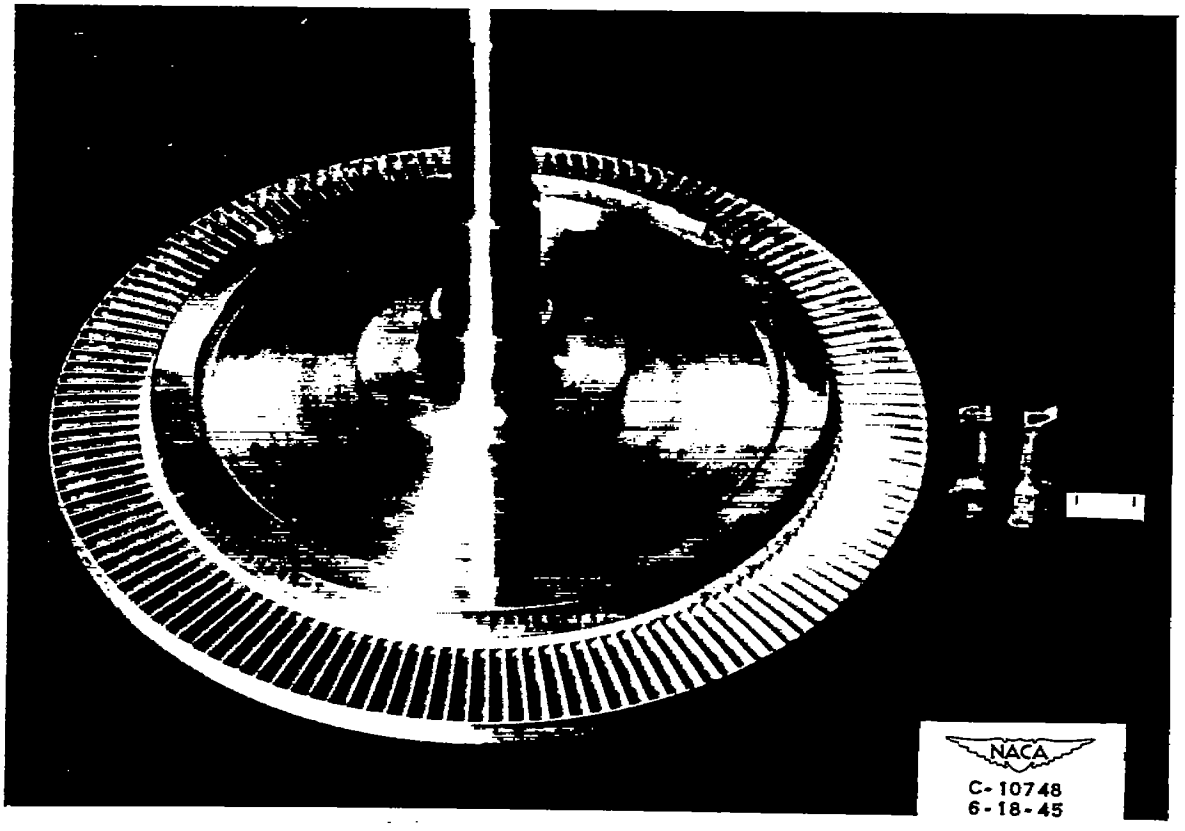

Figure 3. - Photograph of assembled rotor showing rotating cylindrical shroud formed by blade caps.

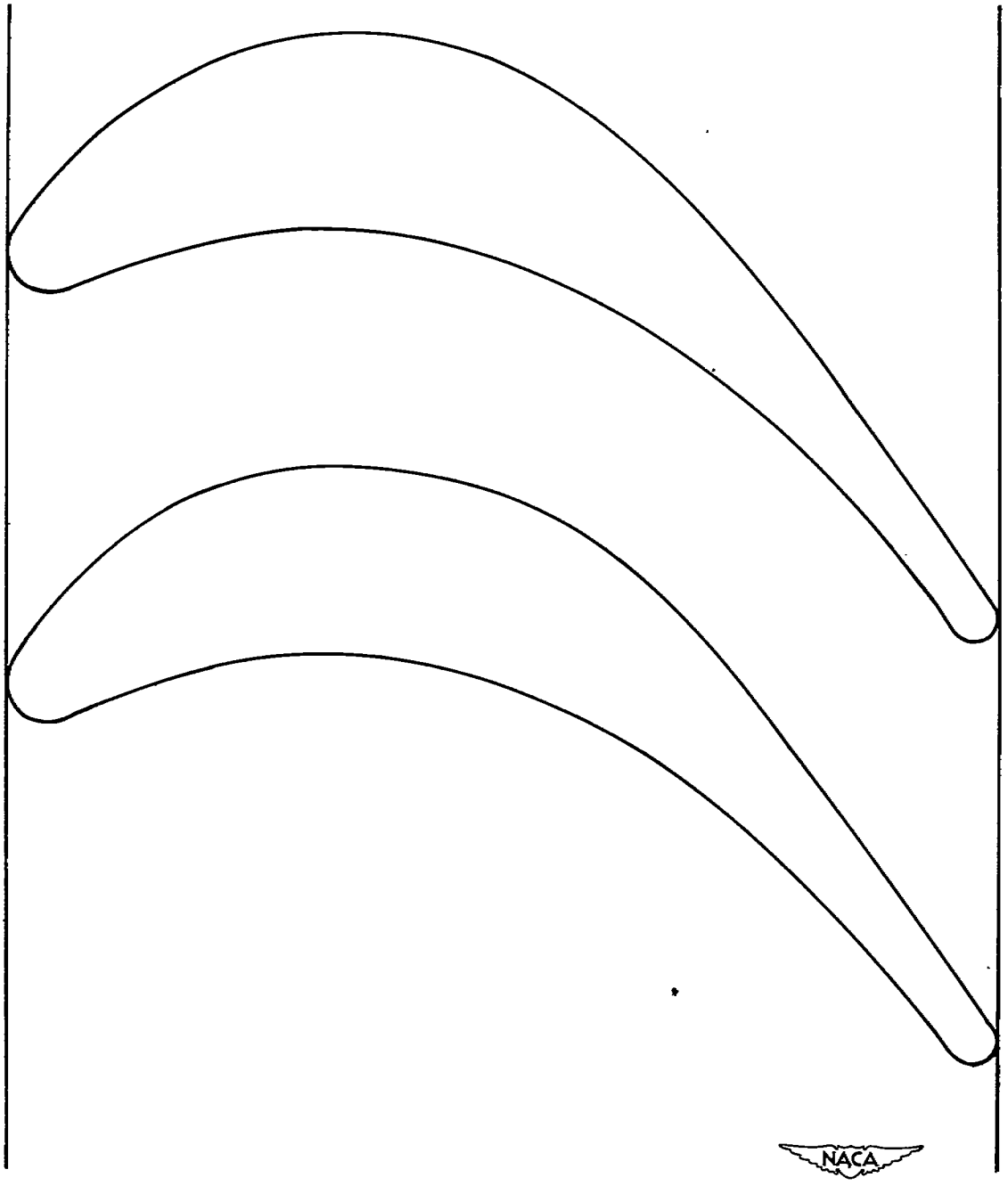

Figure 4. - Diagram showing rotor-blade profile (mean section).

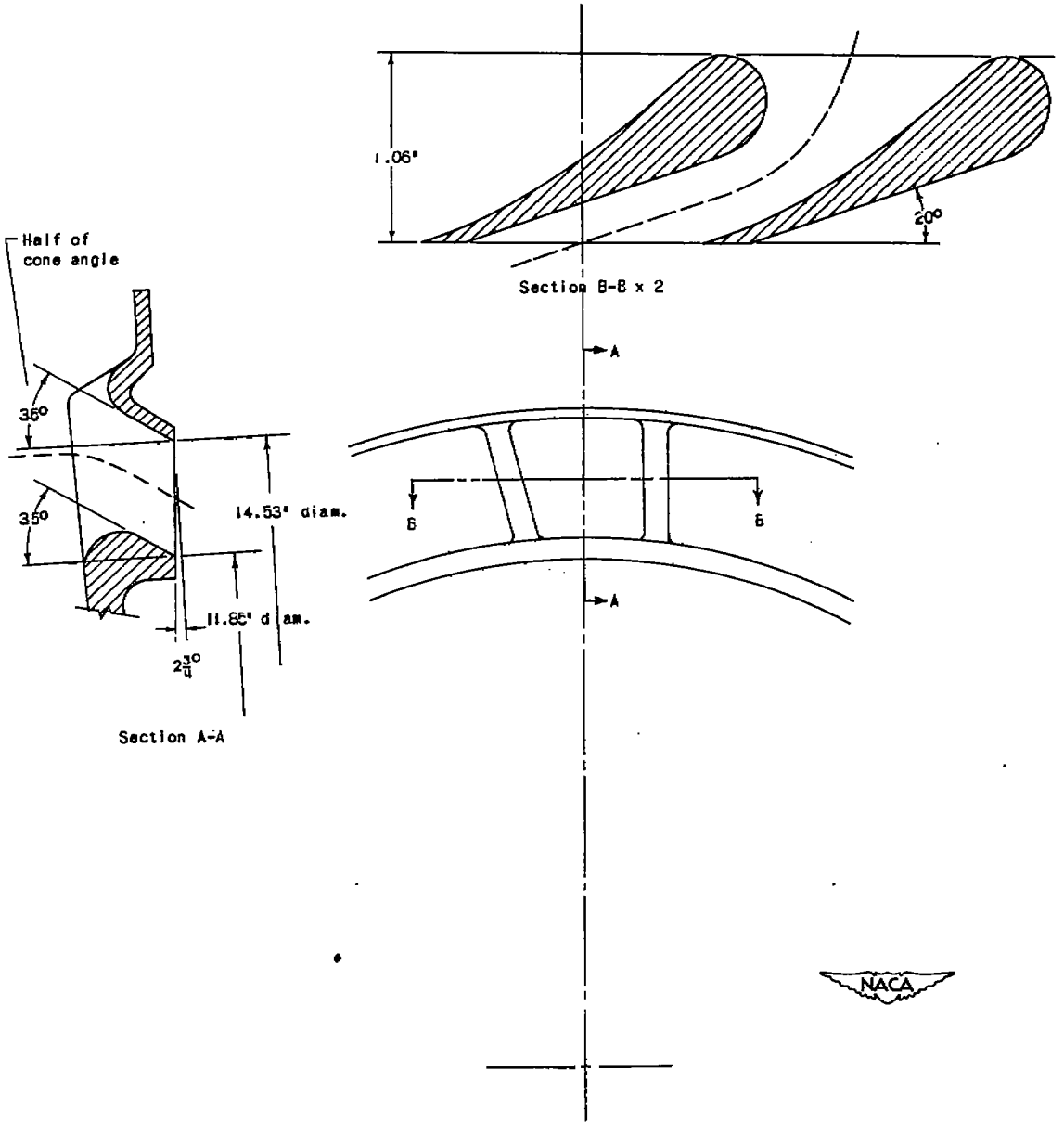

Figure 5. - 70°-cone-angle turbine stator; 28 stator blades.

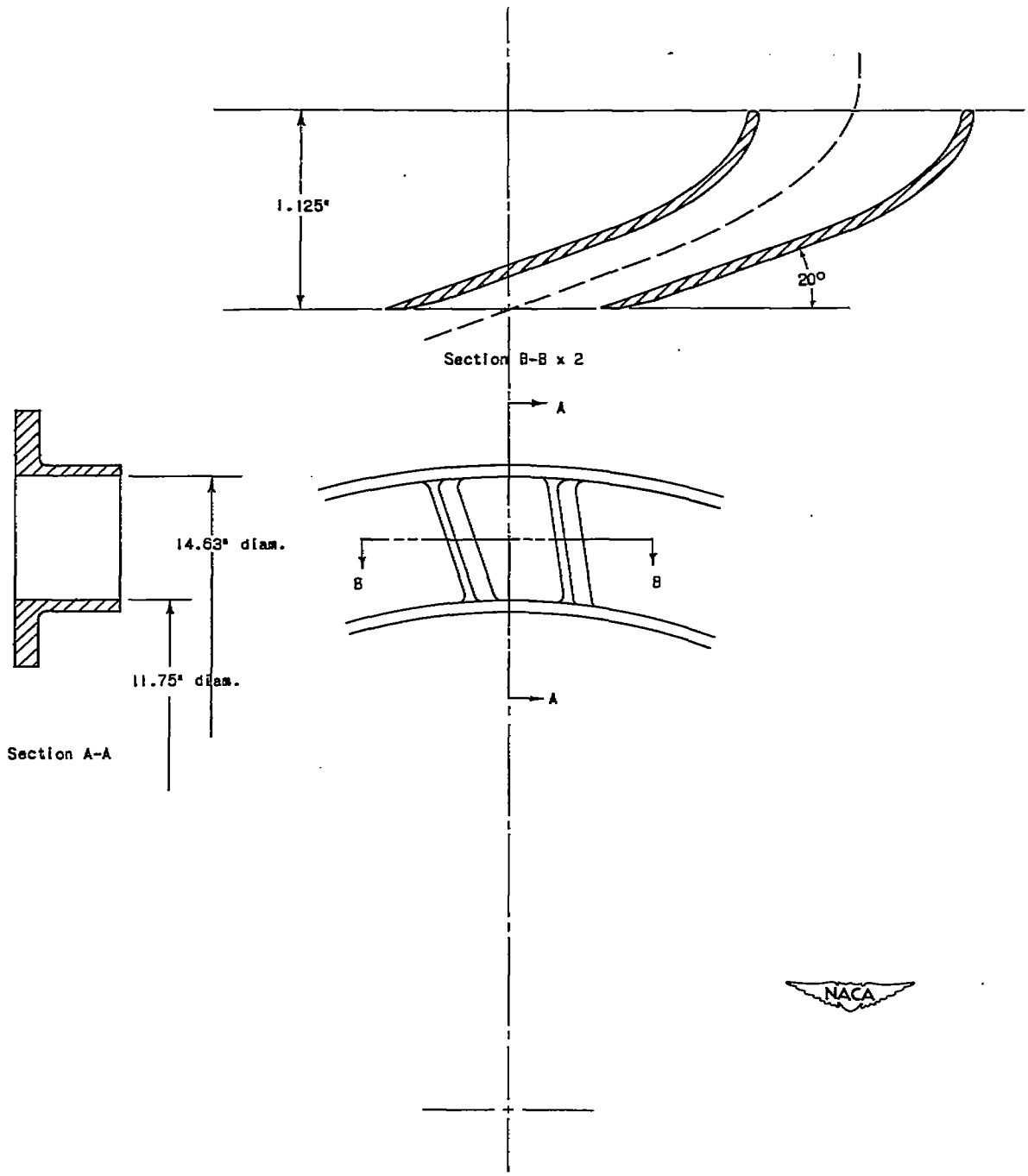

Figure 8. - 0°-cone-angle turbine stator; 36 stator blades.

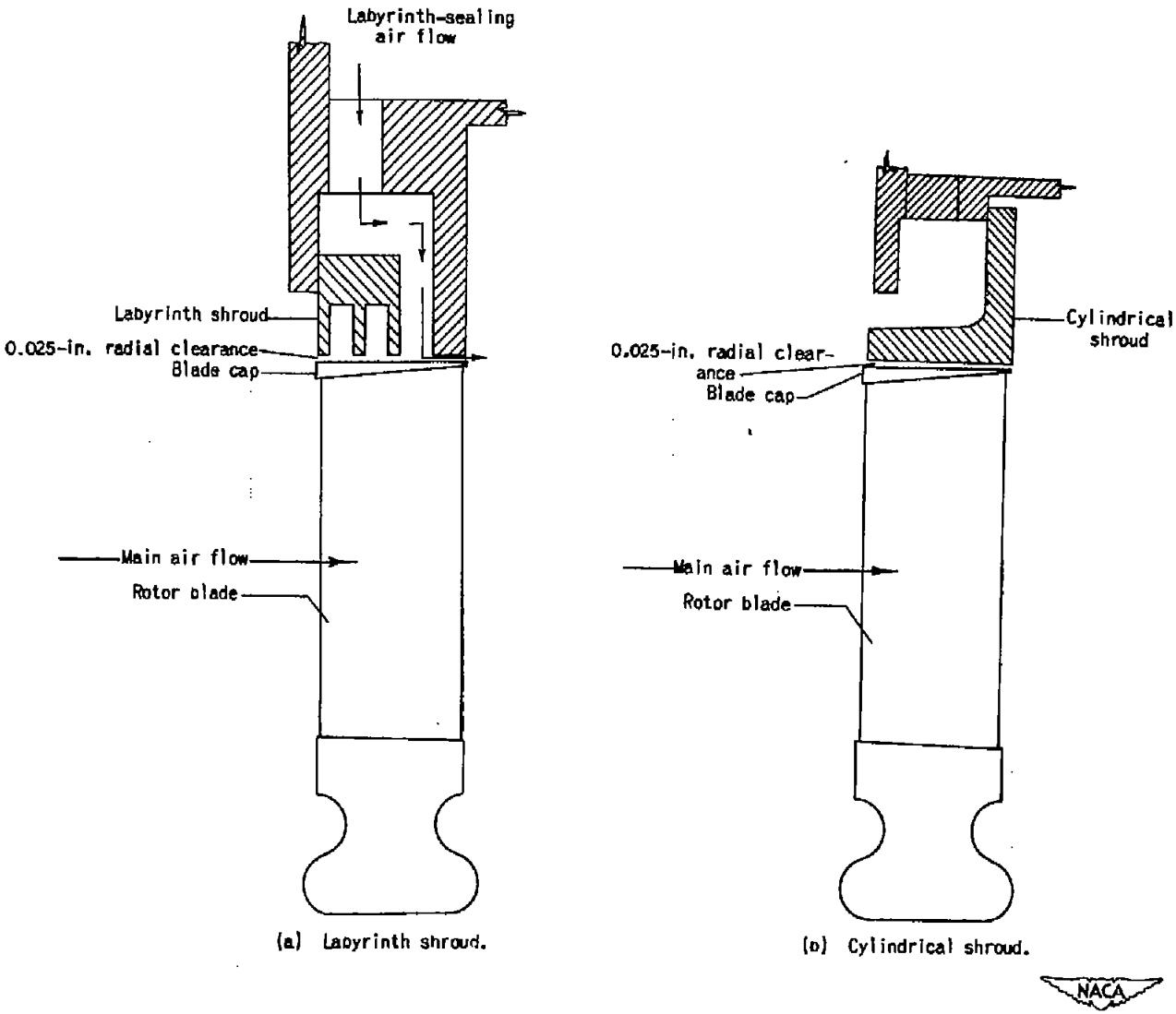

Figure 7. - Installation of stationary shrouds showing labyrinth-sealing air-flow path and radial clearance.

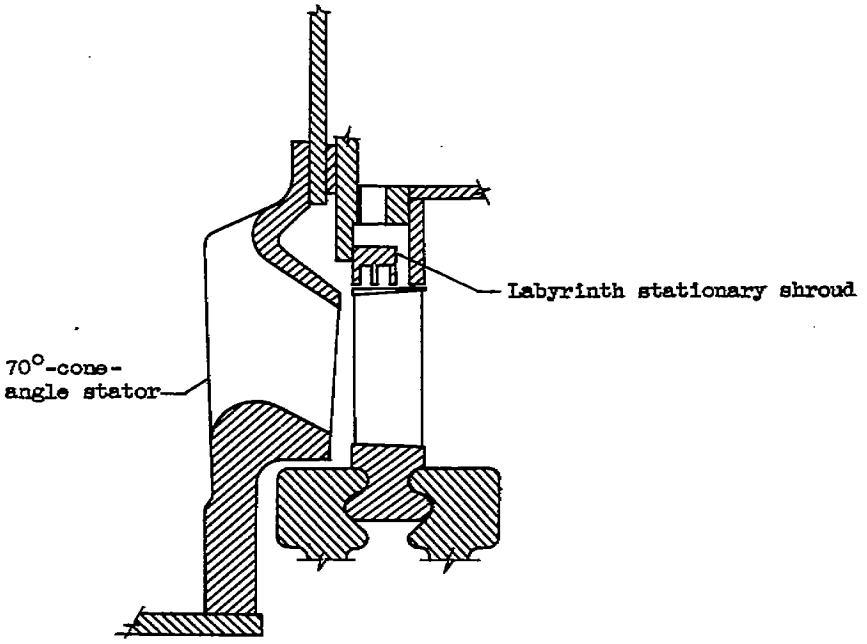

(a) Configuration 1.

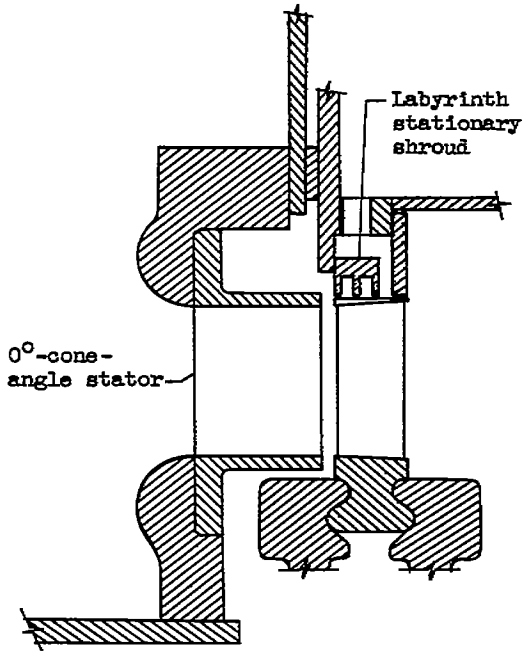

(b) Configuration 2.

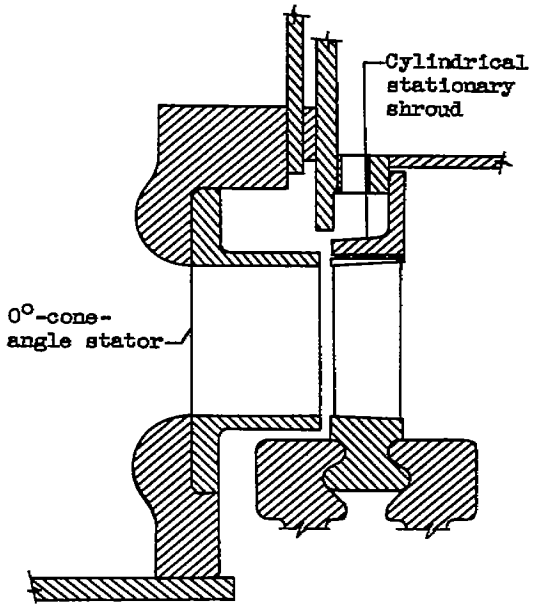

(c) Configuration 3.

NACA

Figure 8. - Three turbine configurations investigated.

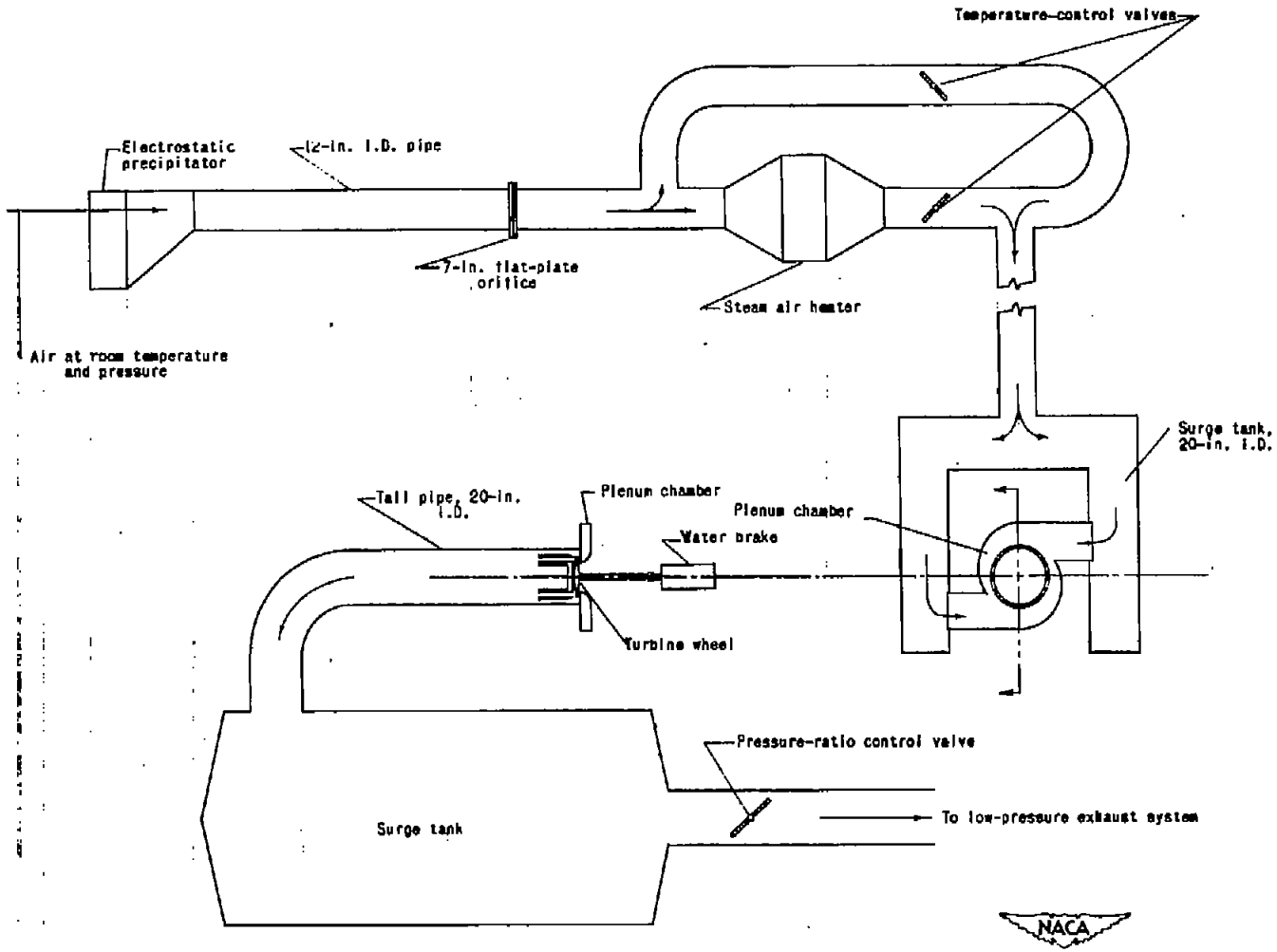

Figure 9. - Diagrammatic sketch of experimental-equipment arrangement showing pressure-ratio control valve, air-flow path, and auxiliary equipment.

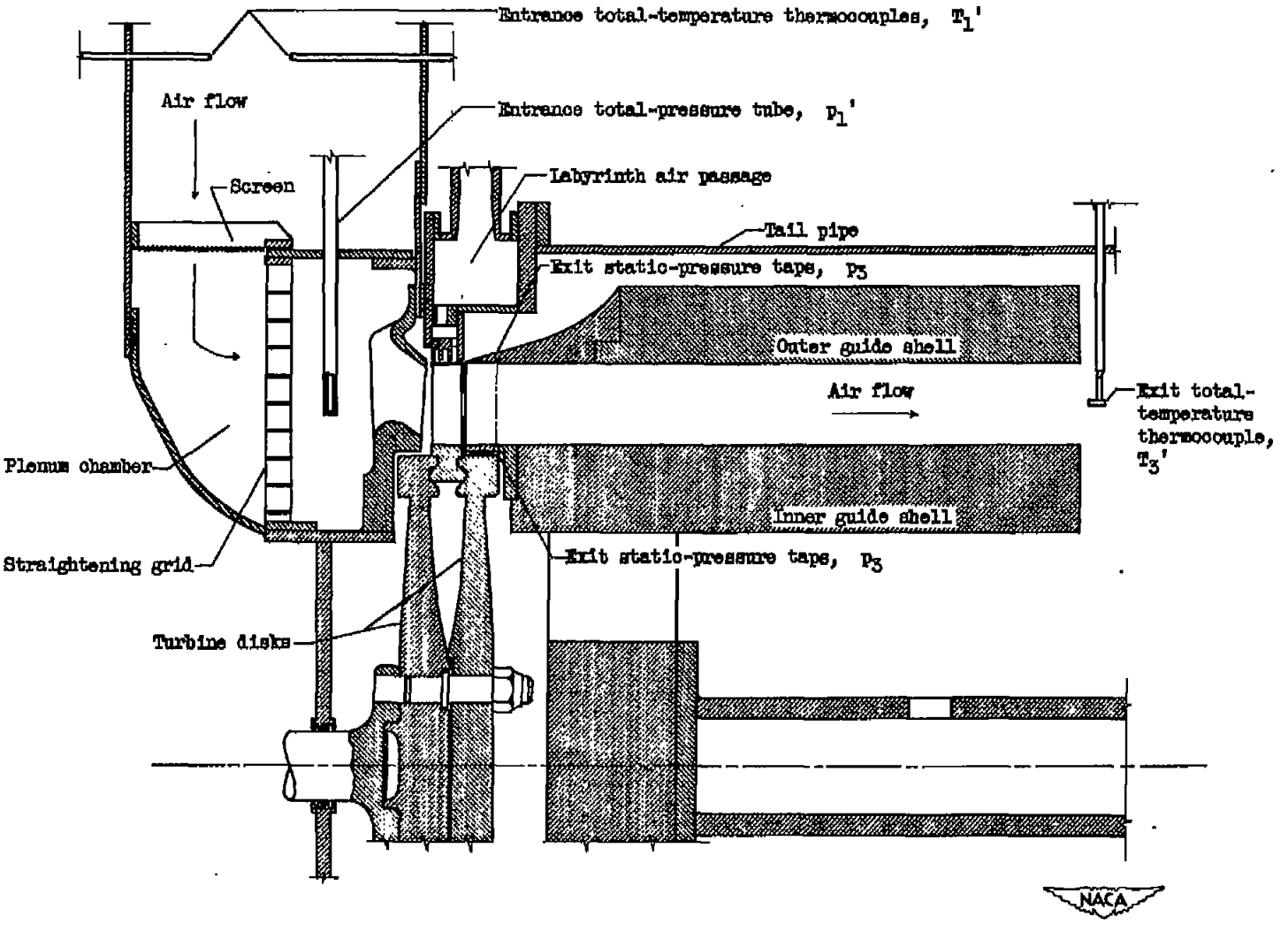

Figure 10. - Cross section through turbine center line (configuration 1) showing turbine arrangement and instrumentation.

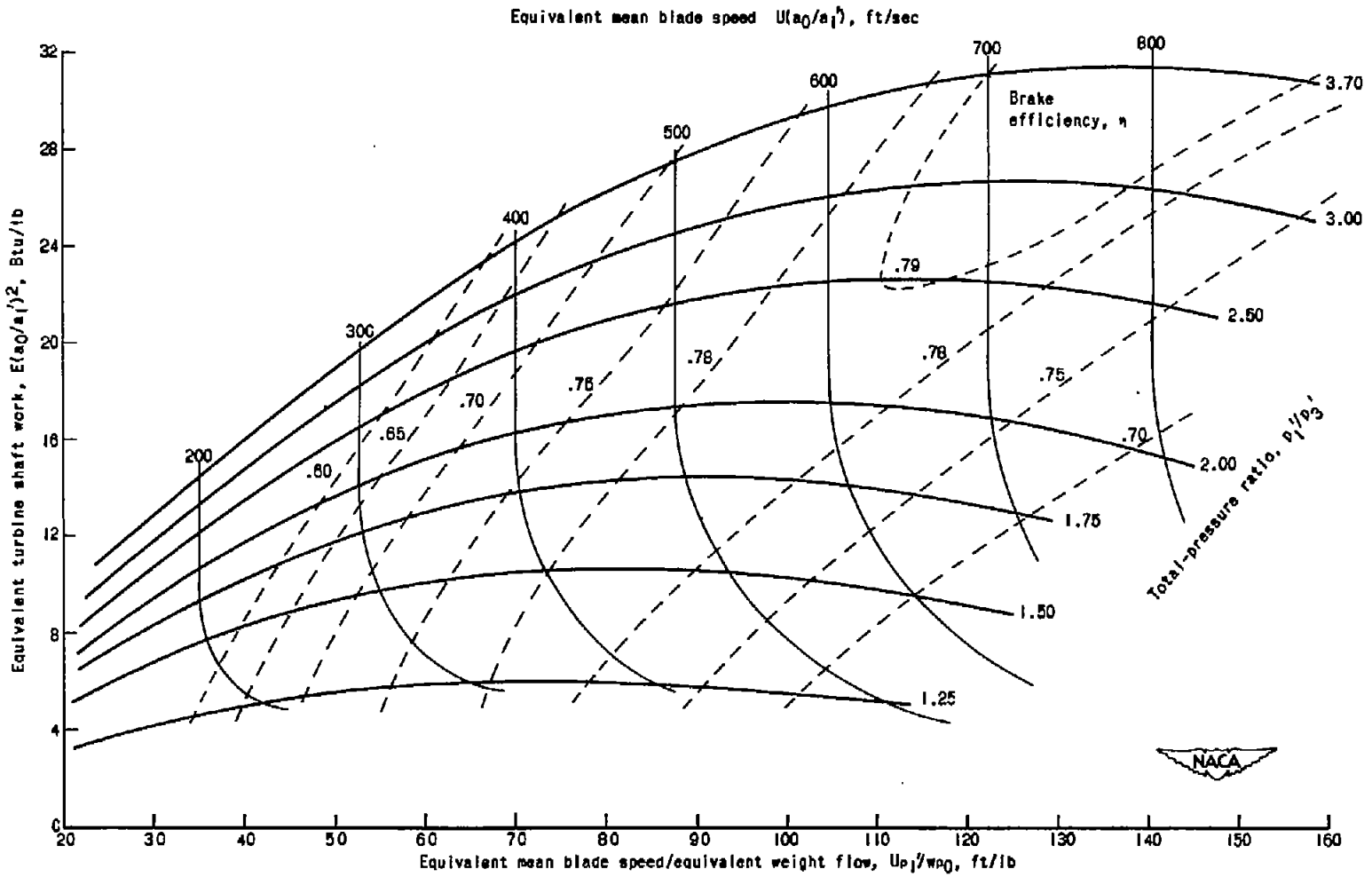

Figure 11. - Over-all performance chart with 70°-cone-angle stator and labyrinth shroud (configuration 1).

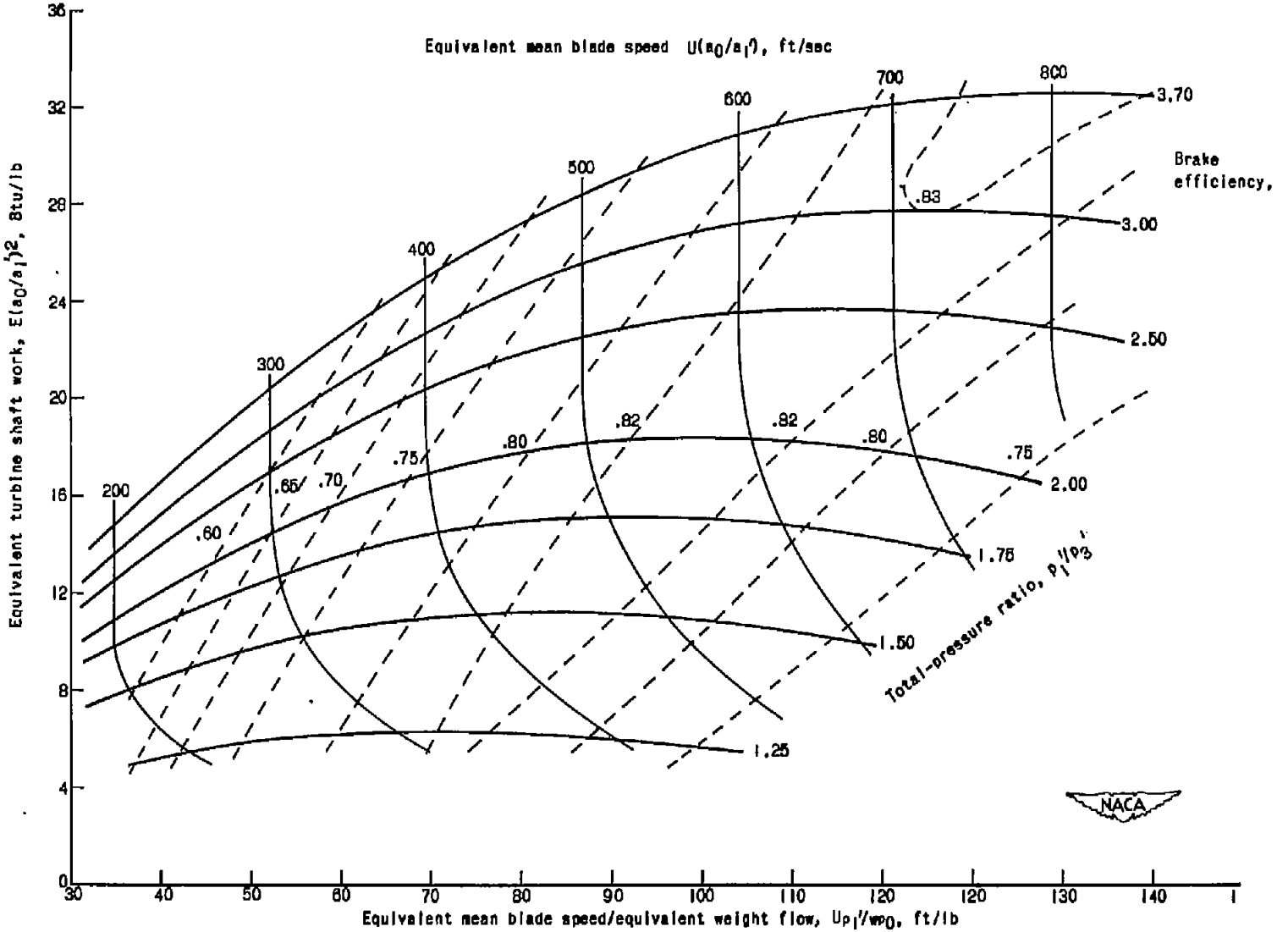

Figure 12. - Over-all performance chart with 0° cone-angle stator and labyrinth shroud (configuration 2).

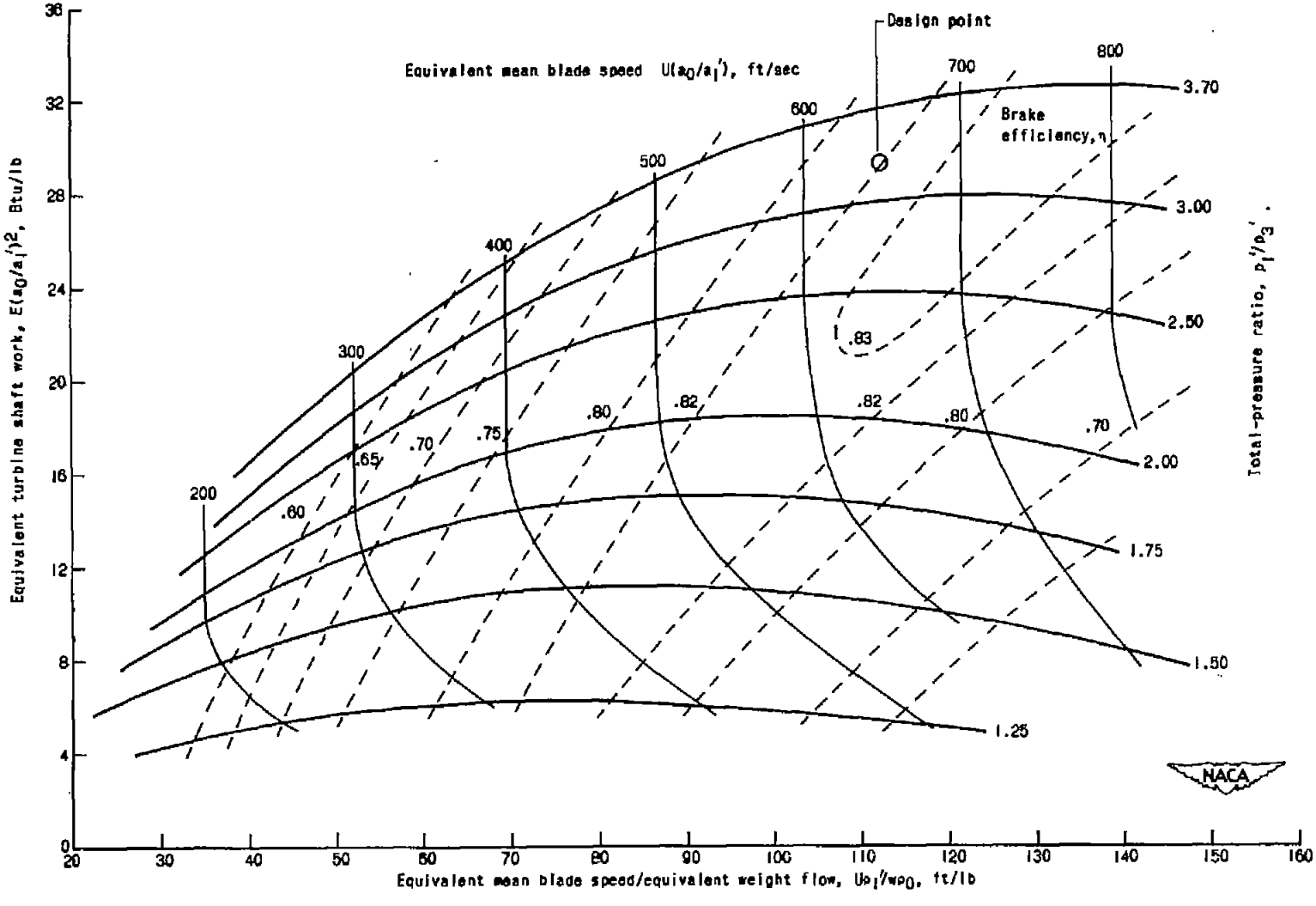

Figure 13. - Over-all performance chart with 0° cone-angle stator and cylindrical shroud (configuration 3).

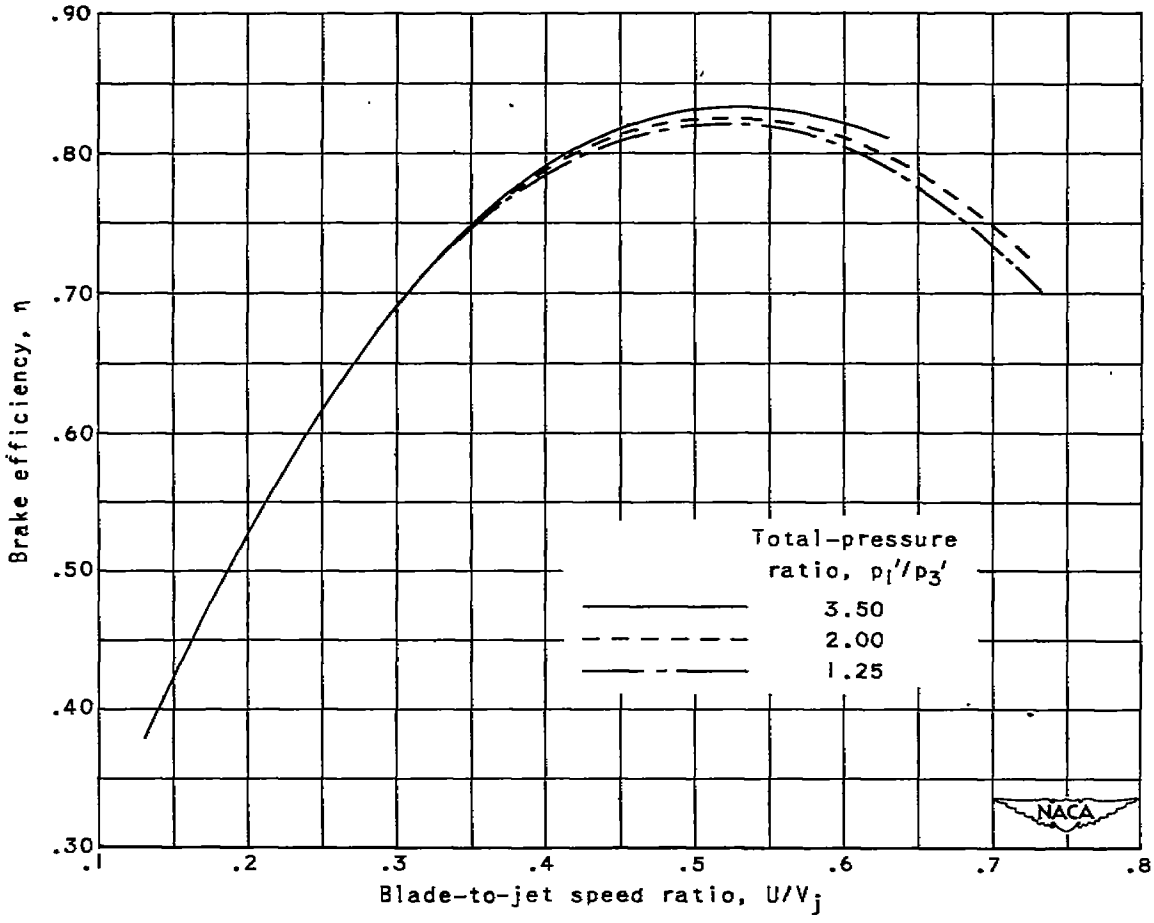

Figure 14. – Efficiency of configuration 2 at various pressure ratios.

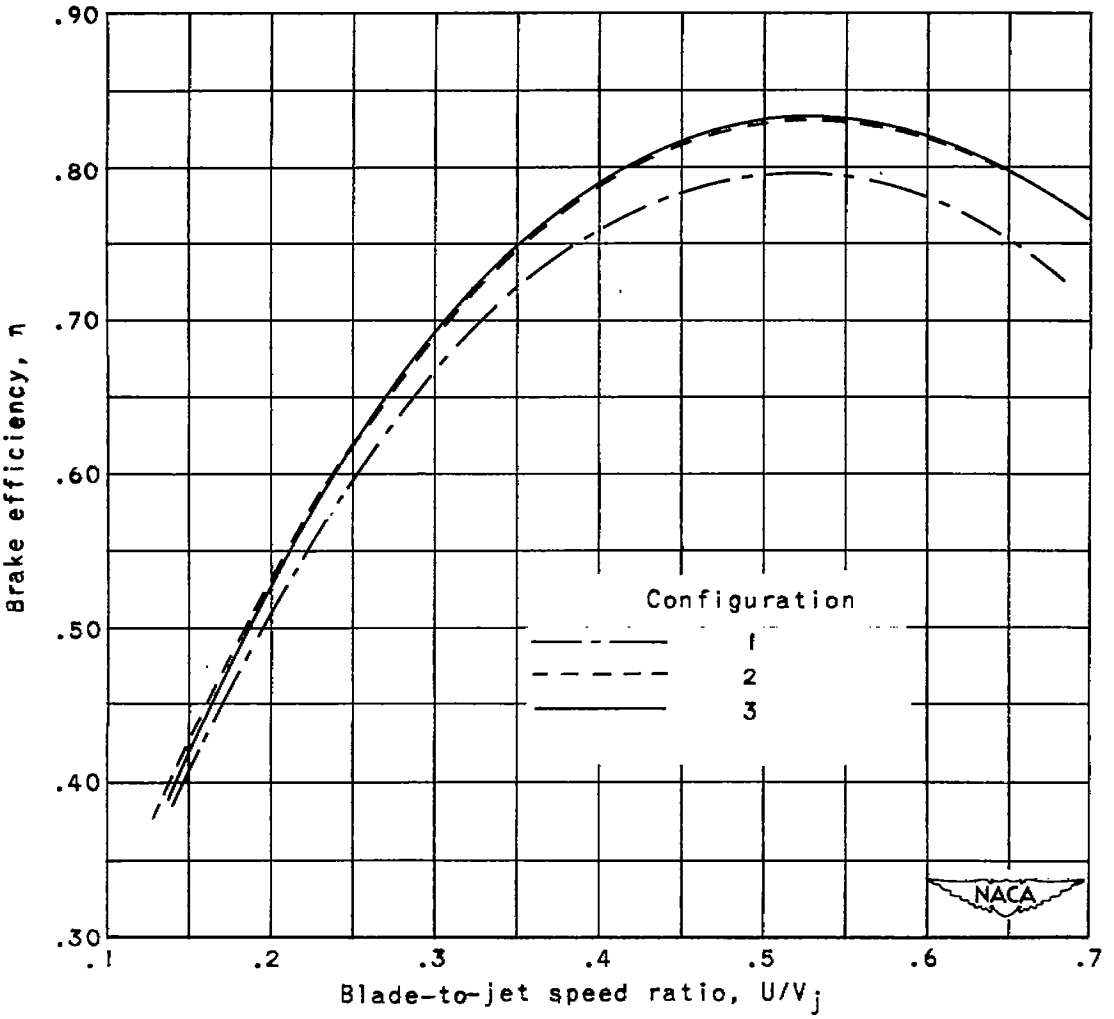

Figure 15. - Comparison of configurations 1, 2, and 3 at a total-pressure ratio of 3.00.